IMPROVED RELIABILITY THROUGH THE USE OF DESIGN AUDITS

by

J. C. Wachel

President

Kenneth E. Atkins

Senior Staff Engineer

and

James D. Tison

Senior Staff Engineer

Engineering Dynamics Incorporated

San Antonio, Texas

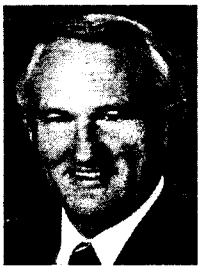

J.C. (Buddy) Wachel is President of Engineering Dynamics Incorporated, an independent consulting firm. He has over 36 years of experience and has published over 40 technical papers. He has solved problems worldwide in piping vibrations, lateral and torsional critical speeds, rotor instabilities, and crankshaft failures. In addition to the practical field experience, he supervises the computer design audits of machinery and piping to ensure that the systems will have acceptable vibrations and stresses. He has B.S.M.E. and M.S.M.E. degrees from the University of Texas. He is an ASME Fellow and a member of ASM, The Vibration Institute, and is a registered Professional Engineer in the State of Texas.

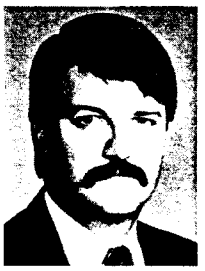

Kenneth E. (Ken) Atkins is a Senior Staff Engineer with Engineering Dynamics Incorporated and has experience in performing lateral and torsional critical speed analyses, rotor stability analyses, and the evaluation of structural vibration problems using finite element methods. He has been actively involved in field troubleshooting of a wide variety of rotordynamics, structural, and piping vibration problems. Mr. Atkins received a B.S. degree (Engineering) from Trinity University (1978). He is a member of ASME and a registered Professional Engineer in the State of Texas.

James D. (Jim) Tison is a Senior Staff Engineer at Engineering Dynamics Incorporated. He has been extensively involved in field measurements and computer modelling of rotating and reciprocating equipment for over 17 years. For 12 years, his work has been primarily related to development and improvement of software for the simulation of pulsation in compressor and pump piping systems, and overall responsibility for acoustic and mechanical design studies of reciprocating compressor and pump piping systems. He is a member of ASME and holds B.S. and M.S. degrees (Mechanical Engineering) from the University of Florida.

ABSTRACT

Rotordynamic design audits of machinery and systems can be used to identify potential problems before manufacture, thus preventing costly project delays and downtime. Machinery engineers need to understand the types of analyses that can be performed to evaluate proposed designs. Understanding the analysis types can also help the engineer to determine if the audit is necessary and/or economically desirable. The types of audits that should be performed are described. Typical analysis results are presented along with guidelines for their interpretation.

INTRODUCTION

The decision to perform an independent rotordynamic design audit is generally based on the type of machine, the manufacturer's experience with machines of similar size, speed, etc., and the assessment of the benefits *vs* the cost of the analysis. If it could be assumed that nothing would go wrong, then a design audit would not be needed. However, experience shows that design and manufacturing problems do occur that can result in considerable delay to projects. Cook [1] indicates that over half of the major expansion projects from 1976 to 1986 encountered a critical speed problem and/or high vibration near rated speed. This study indicated that the delay time to correct design equipment error could be as high as 100 weeks. For some performance design error problems, up to four years were needed to correct the problems.

Bloch [2] states that approximately 22 percent of the unscheduled downtime events for major turbocompressors in process plants are caused by the rotor/shaft systems. Considering all the unscheduled downtime causes that could be vibration-related, the percentage would be greater than 50 percent. A study by an insurance company found that failures expected each year were about one out of every 186 for steam turbines, and one out of every 26 for gas turbines [2].

Data such as this, and the authors' experience in troubleshooting vibration and failure problems, indicate that design audits can help prevent many of the problems that cause unscheduled downtime, project delays, and/or failures, by identifying potential problem areas before startup [3]. Most major turbomachinery manufacturers have the necessary capabilities for evaluating rotordynamic designs. However, many user companies prefer an independent design audit, particularly when a system consists of machinery components from various manufacturers.

Another reason for performing an independent audit is the fact that the system may consist of used equipment. In order to avoid any contractual liabilities, the OEM may not v want to perform the rotordynamic calculations on revamped systems or the chang-

es that are being made. Discussion here is limited to the types of rotordynamic analyses that are commonly performed, the technology available, and will present typical audit report formats. An outline of the major types of rotordynamic design audits that are typically performed is presented in Table 1.

Table 1. Outline of Major Design Audits.

1. Lateral Critical Speed Analyses
   - Critical Speed Map
   - Undamped Natural Frequencies
   - Undamped Mode Shapes
   - Bearing and Seal Stiffnesses and Damping
   - Rotor Response to Unbalance
   - Pedestal and Foundation Effects on Response
   - Stability
2. Torsional Critical Speed Analyses
   - Natural Frequencies
   - Mode Shapes
   - Interference Diagram
   - Coupling Dynamic Torques
   - Dynamic Gear Loads
   - Harmonic Torque Loads for Reciprocating Machinery
   - Torsional Vibrations
   - Shaft Stresses
3. Transient Torsional and Variable Frequency Drive Analyses
   - Start Up Time
   - Stress Versus Time
   - Cumulative Fatigue
   - Allowable Number of Starts
   - Electrical Shorts
4. Impeller and Blade Analyses
   - Natural Frequencies
   - Mode Shapes
   - Interference Diagram
   - Experimental Shaker Tests or Modal Analysis

LATERAL CRITICAL SPEED ANALYSIS

The most common rotordynamic design audits are lateral and torsional critical speed analyses. Experience indicates that many systems have been installed with critical speeds in the running speed range and have run successfully for years before troubles were encountered. These problems are sometimes difficult to understand, but a design audit that considers the entire range of possible values for critical system parameters will usually identify the potential for problems to occur.

A lateral critical speed analysis should include the following calculations:

- Critical speed map
- Undamped natural frequencies and mode shapes
- Bearing stiffness and damping properties
- Seal stiffness and damping properties
- Rotor response to unbalance
- Rotor stability
- Pedestal and foundation effects on response and stability

The first step in performing a lateral critical speed analysis is to model the shaft with sufficient detail to accurately simulate the rotor response throughout its speed range. An accurate drawing giving the shaft dimensions, weights, and centers of gravity for all added masses is required to develop the model. Generally, each significant shaft diameter change is modelled by one or more stations. A station is generally located at each added mass or inertia, at each bearing and seal location, and at each potential unbalance location. A typical rotor shaft drawing and the corresponding computer model is illustrated in Figure 1.

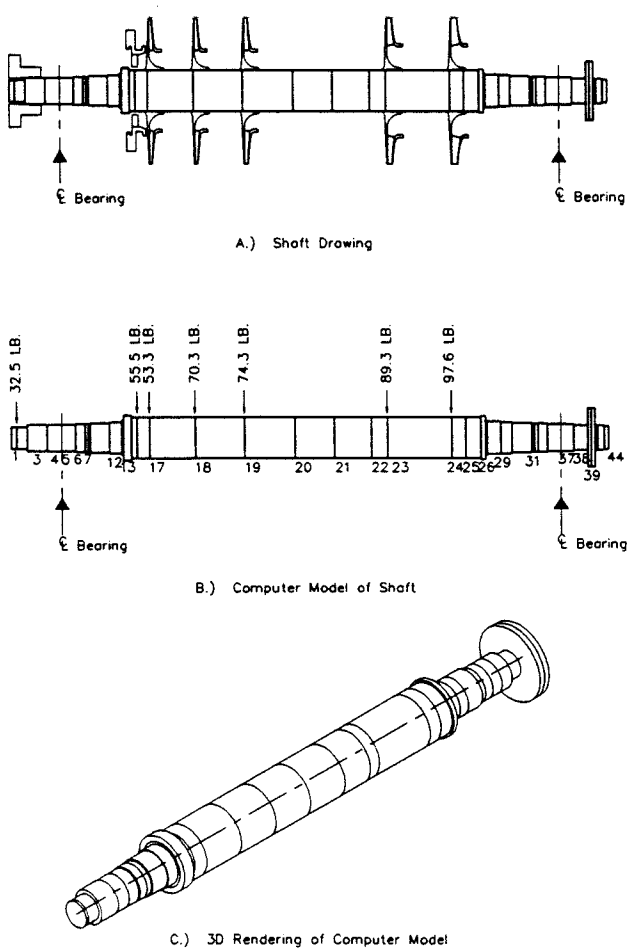

Figure 1. Rotor Model for Lateral Critical Speed Analysis.

Rotating elements such as wheels and impellers are modelled as added masses and inertias at the appropriate locations on the shaft. The polar and transverse mass moments of inertia are included in the analyses to simulate the gyroscopic effects on the rotor. The gyroscopic effects are particularly significant for overhung rotors, since the impeller or disk produces a significant restoring moment when whirling in a deflected position.

Couplings are also simulated as concentrated added masses and inertias. Normally, half of the coupling weight is placed at its center of gravity. For most turbomachinery systems, flexible couplings effectively isolate the lateral vibrations of adjacent rotors. Therefore, each rotor can usually be analyzed independent of the coupled rotors. However, if the couplings do not isolate the rotors, the entire train, including the driver and driven equipment, should be modelled.

Analysis Methods

There are numerous computational methods that are used to analyze lateral vibration of rotors. Transfer matrix based methods have probably been the most widely used technique. This method minimizes required computer resources (memory, speed,

etc.). However, the iterative technique for solution of the eigenvalue problem used in conjunction with this method has the disadvantage of not guaranteeing the determination of all eigenvalues. Even important lower frequency eigenvalues can be missed.

A general-use rotordynamics code has been developed by EDI which is based on matrix methods. The mass ([*M*]), stiffness ([*K*]) and damping ([*C*]) matrices, which are coefficients of the system differential equation

$$[M]\{\ddot{x}\} + [C]\{\dot{x}\} + [K]\{x\} = \{F\}, \qquad (1)$$

are determined based on the input rotor model, bearing, and seal parameters, and forcing functions. These matrices are the building blocks for the two fundamental mathematical formulations required for rotordynamic analysis:

- The eigenvalue problem
- Unbalanced (forced) response

The eigenvalue problem is formulated from Equation (1) by reduction of order with $x_2 = \dot{x}_1$ to obtain:

$$\begin{Bmatrix} (\dot{x}_2) \\ (\dot{x}_1) \end{Bmatrix} = [A] \begin{Bmatrix} (x_2) \\ (x_1) \end{Bmatrix}$$

where $$[A] = \begin{bmatrix} -[M]^{-1}[C] & -[M]^{-1}[K] \\ [I] & [0] \end{bmatrix}$$

The eigenvalues and eigenvectors are determined from the dynamic matrix [*A*]. The eigenvalue solution is used for the rotor stability calculation. The real part of the eigenvalue determines the stability characteristics and the imaginary part determines the vibratory frequency of the mode. A commercially available eigenvalue solver is used to obtain the eigenvalues and mode shapes (eigenvectors).

The unbalanced response problem uses Equation (1) above with:

$$\{F\} = w^2\{U_c\}\cos wt + w^2\{U_s\} \sin wt \qquad (2)$$

where $\{U_c\}$ and $\{U_s\}$ are the constant amplitude excitation vectors.

Assuming the usual solution form

$$\{x\} = \{a\} \cos wt + \{b\} \sin wt, \qquad (3)$$

Substitution into Equation (1) gives the system of linear equations of the form [A] {x} = {b}.

$$\begin{bmatrix} [K] - w^2[M] & w[C] \\ -w[C] & [K] - w^2[M] \end{bmatrix} \begin{Bmatrix} (a) \\ (b) \end{Bmatrix} = w^2 \begin{Bmatrix} (U_c) \\ (U_s) \end{Bmatrix}$$

The forced response problem is, therefore, reduced to the solution of a system of linear equations that is solved very rapidly using a sparse matrix solution technique.

Overall, this matrix technique provides all of the required types of rotordynamic calculations. Some of the major attributes of the code are:

- Solution of both eigenvalue (damped and undamped) and forced response in a single code.
- All eigenvalues are determined (no roots are missed).
- Principal and cross coupled mass terms, as well as stiffness and damping terms, are allowed at bearing stations.
- Pedestal mass and flexibility (at bearing stations) are modelled.
- Numerical problems associated with the classical transfer matrix techniques are not inherent.
- Matrix based formulation facilitates simple addition of element type for substructures.
- Input data is organized in modules to facilitate convenient use of code for different tasks and/or parametric cases.
- Powerful post processors have been developed to aid in the visualization of rotor mode shapes and forced vibration response.

The classical matrix method discussed by Childs [4] and Crandall [5] has been, in the past, deemed too slow computationally for practical use. However, with the use of efficient matrix solvers in conjunction with the increased speed of today's computers, the method has been proven to have several advantages over the transfer matrix program. The code, written in FORTRAN, is run on an HP series 735 workstation, with a typical time to solution for a 50 mass station model ranging from 0.3 minutes for unbalance response calculations, to 2.0 minutes for stability calculations for multiple aerodynamic loading cases.

Critical Speed Map

The critical speed map is a logarithmic plot of the undamped lateral critical speeds *vs* the combined support stiffness, consisting of the bearing and support structure as springs in series. The critical speed map provides useful information for understanding the basic response behavior of rotors; therefore, it is important to understand how the map is developed.

A "normalized" critical speed map is shown in Figure 2, to illustrate the relationships of the various critical speeds for low and high support stiffness values, and to illustrate the mode shapes that the rotor will have at different bearing and support stiffness values. For the "rigid bearing" critical speeds ($K_{support} >> K_{shaft}$), the mode shape for the first mode is a half-sine wave (one loop). The second critical speed is a two loop mode and would occur at four times the frequency of the first mode critical, the third critical speed is a three loop mode and would be nine times the frequency of the first critical, etc. Obviously, for real rotor systems, the bearing stiffnesses are finite. The second critical speed is typically two to three times the first critical, but cannot be more than four times the first, even for rigid bearings.

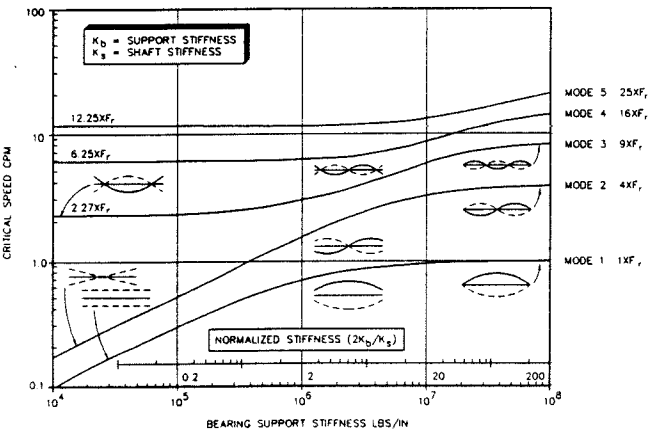

Figure 2. Normalized Critical Speed Map.

For low values of support stiffness $K_{shaft} >> K_{support}$, the first critical speed is a function of the square root of the total rotor weight and the sum of the two support spring stiffnesses. For an ideal long slender beam, the second mode is similar to the rocking of a shaft on two springs, and is equal to 1.73 times the first critical speed. Since both the first and second modes are a function of the support stiffness, the slope of the frequency lines for the first and second critical speeds *vs* support stiffness is proportional to the square root of the stiffness for low values of support stiffness compared to the shaft stiffness.

For a support stiffness of zero, the third and fourth modes would be analogous to the first and second free-free modes of a beam. For an ideal uniform beam, the ratio of the frequencies for these modes compared to the first critical speed for rigid bearings is 2.27 and 6.25.

The normalized critical speed is based on ideal beam theory and is a useful beginning for understanding rotor vibration. Actual rotors differ from ideal beams in that rotor vibration consists of the shaft precessing or whirling in its supports instead of simple lateral motion. This occurs while the shaft is spinning at its rotational speed. Rotor vibration (whirl) can occur at the same speed as the spin frequency(synchronous) or at some other nonsynchronous frequency. The rotor can precess in the same direction as rotation (forward whirl) or opposite rotation (backward whirl).

An actual critical speed map for a five stage compressor is shown in Figure 3. Note that both forward and backward whirl modes are shown on the map. Curves representing bearing stiffness are superimposed on the map. Intersections between the bearing stiffness curves and the mode curves (circled on Figure 3) represent undamped critical speeds.

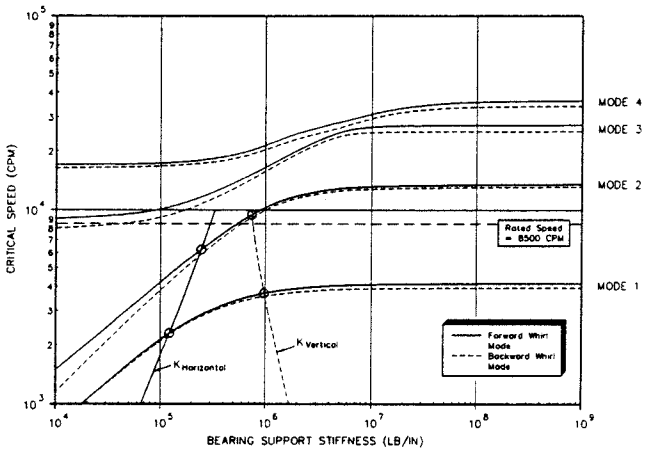

Figure 3. Critical Speed Map for Five Stage West Gas Compressor.

Bearing Stiffness and Damping

The dynamic stiffness and damping coefficients of fluid film bearings can be adequately simulated using eight linear coefficients (K_{xx}, K_{yy}, K_{xy}, K_{yx}, C_{xx}, C_{yy}, C_{xy}, C_{yx}), (Figure 4). This information, along with the lubricant minimum film thickness, flow, power loss, and temperature rise at operating conditions, is needed to evaluate the bearing design. The bearing stiffness and damping coefficients are calculated as functions of the Sommerfeld number(s), which are defined as:

$$S = \frac{\mu N D L}{W} \left(\frac{R}{C}\right)^2 \qquad (4)$$

where:
μ = lubricant viscosity, lb-sec/in
N = rotor speed, Hz
D = bearing diameter, in
L = bearing length, in
R = bearing radius, in
W = bearing load, lbs
C = radial machined clearance, in

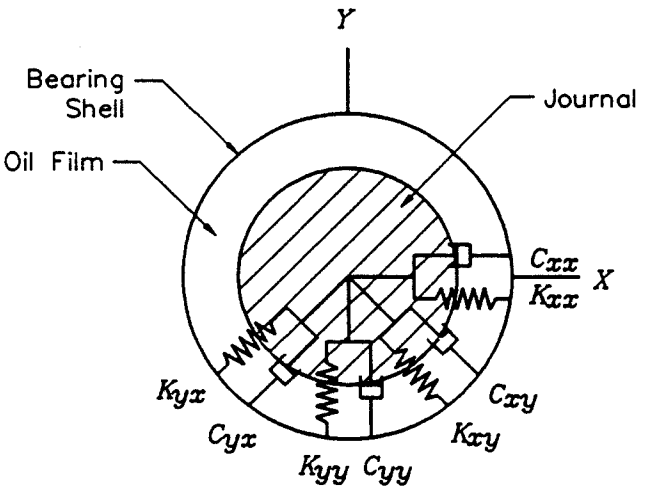

Figure 4. Bearing Stiffness and Damping Coefficients.

Several authors [6, 7, 8, 9, 10] discuss various types of bearings and their stiffness and damping characteristics. A typical set of bearing calculations for a five shoe, load on pad, tilting pad bearings is shown in Table 2. The actual stiffness and damping values as well as power loss, oil flow, viscosity, and oil film temperature and thickness are shown *vs* speed and eccentricity ratio.

Table 2. Bearing Coefficients for Tilting Pad Bearing.

5 SLOP Bearing Example - Nominal Dimensions
Wet Gas Compressor - Drive End Bearing

Load on Pad L/D= 0.39 Preload= 0.421
Arc Length = 56 Deg. Pad Angle = 54 Deg. Offset = 0.5

L= 1.625 in D= 4.126 in Load= 595 lbs Load/(L*D)= 88.8 psi
T_{in} = 120 Deg F Assembled Clearance = 9.5 mils Diametral
Machined Clearance = 5.5 mils Diametral
Inlet Oil Viscosity= 2.49E-06 lb-s/in^2
Density= 8.08E-05 lb-s^2/in^4

ECC (Dim)	Speed (RPM)	Kxx (lb/in)	Kyy (lb/in)	Cxx (lb-s/in)	Cyy (lb-s/in)	Power Loss (HP)	Total Circ Oil Flow (Gal/Min)	Average Viscosity (Reyns)	Average Film temp (Deg F)	Reynolds Number (Dim)	Min Film (mil)
0.828	500	4.04E+04	2.16E+06	7.04E+02	1.18E+04	0.04	3.86E-01	1.56E-06	144	2.33E+01	0.33
0.764	1000	6.51E+04	1.68E+06	6.58E+02	6.20E+03	0.11	6.92E-01	1.55E-06	144	4.17E+01	0.48
0.611	3000	1.50E+05	1.05E+06	5.47E+02	1.89E+03	0.72	2.11E+00	1.47E-06	147	1.32E+02	0.86
0.522	5000	2.13E+05	8.73E+05	4.88E+02	1.15E+03	1.75	3.53E+00	1.41E-06	150	2.29E+02	1.08
0.458	7000	2.65E+05	7.90E+05	4.48E+02	8.54E+02	3.16	4.96E+00	1.36E-06	152	3.33E+02	1.24
0.428	8200	2.93E+05	7.62E+05	4.30E+02	7.47E+02	4.18	5.82E+00	1.33E-06	153	3.98E+02	1.32
0.410	9000	3.11E+05	7.48E+05	4.19E+02	6.93E+02	4.92	6.39E+00	1.31E-06	154	4.43E+02	1.36
0.390	10000	3.32E+05	7.37E+05	4.07E+02	6.39E+02	5.91	7.10E+00	1.29E-06	155	5.00E+02	1.41

The normal procedure in a design audit is to calculate the bearing characteristics for the range of expected clearances and preload. The maximum clearance and minimum preload usually define the minimum stiffness. The other extreme is obtained from the minimum clearance and maximum preload. This will typically define the range of expected stiffness and damping coefficients for the bearings. An example is given in Table 3 of the bearing clearances and preloads that can be obtained by considering the dimensional tolerances for the shaft and bearing.

Table 3. Clearance and Preload Variations with Tolerances.

	Minimum	Maximum
Bearing Assembled Diameter (D_a)	4.130	4.133
Bearing Machined Bore (D_m)	4.134	4.137
Shaft Journal Diameter (D_j)	4.125	4.127

D_a (in)	D_m (in)	D_j (in)	Cl_{md} (mils)	Cl_{ad} (mils)	Preload
4.130	4.134	4.125	9	5	0.44
4.130	4.137	4.125	12	5	0.58
4.133	4.134	4.125	9	8	0.11
4.133	4.137	4.125	12	8	0.33
4.130	4.134	4.127	7	3	0.57
4.130	4.137	4.127	10	3	0.70
4.133	4.134	4.127	7	6	0.14
4.133	4.137	4.127	10	6	0.40

Cl_{md} is the machined diametral clearance.
Cl_{ad} is the assembled diametral clearance.

$$\text{Preload} = 1 - Cl_{ad}/Cl_{md}$$

Seal Stiffness and Damping Coefficients

In addition to the bearing stiffness and damping effects, the seals and labyrinths can influence the rotor critical speeds and response. Generally, oil ring seals are designed to float with the shaft, since they are held in place by frictional forces dependent upon the pressure balance force and the coefficient of friction. Lubrication and oil seal systems were discussed by Kirk [11] and Salisbury, et. al. [12]. If the seals lock up, they can add additional stiffness and damping. In such cases, they are treated as additional bearings in the rotordynamic calculations. The seal stiffness and damping coefficients are calculated by assuming that the seals are locked at some eccentricity ratio. Typical values of seal stiffness and damping for centrifugal compressors will be less significant than the bearing; however, in some designs they can change the rotor response characteristics, particularly with respect to stability response.

Undamped Natural Frequencies

If the principal bearing stiffnesses are plotted on the critical speed map (Figure 3), the location of the undamped natural frequencies (critical speeds) are identified. By calculating the bearing stiffness and damping coefficients over the expected range of bearing clearances, preload, and viscosity variation, the anticipated range of critical speeds can be estimated. For rotor systems with tilting pad bearings (that have low cross coupled stiffnesses), the measured critical speeds usually correlate well with these undamped intersections. For fixed-geometry bearings with significant cross coupled stiffness and damping values, the damped critical speeds are usually higher than the undamped critical speeds.

Undamped Mode Shapes

An undamped mode shape is associated with each undamped natural frequency and can be used to describe the rotor vibration characteristics. For a support stiffness of 0.5×10^6lb/in, the mode shapes for the first and second undamped natural frequencies of the example rotor are shown in Figures 5 and 6. The plotted mode shapes were calculated assuming no damping. The actual vibration mode shapes and response frequencies during operation can vary depending upon the unbalance distribution and damping. Three dimensional animation techniques are useful for visualizing these modes and are discussed in the unbalance response section.

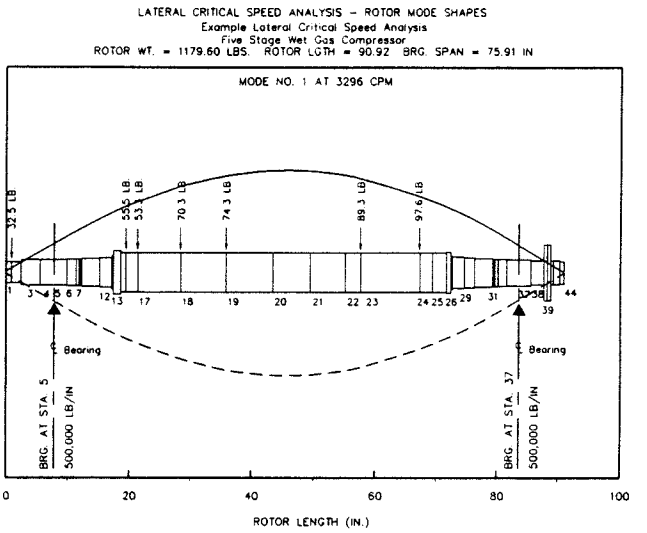

Figure 5. Undamped Mode Shape for First Critical Speed.

Evaluation of Critical Speed Map Calculations

The evaluation of the adequacy of the rotor from the critical speed map and mode shapes should include the following:

- Evaluate the proximity of the critical speed to the running speed or speed range. The undamped lateral critical speeds should not coincide with the running speed. In order to determine if the actual critical speed will cause excessive vibration, it is necessary to perform a rotor unbalance response analysis.

- Assess the location of the critical speed relative to the support stiffness. If the critical speed is near the rigid bearing critical speed (flexible shaft region), increasing the bearing stiffness will not increase the critical speed. Also, vibration amplitudes will be low at the bearings and, therefore, bearing damping will be ineffective. This can contribute to rotordynamic instabilities, which will be discussed later. If the critical speeds are in the area of low support stiffness (stiff shaft region), the critical speeds are strongly dependent upon the bearing

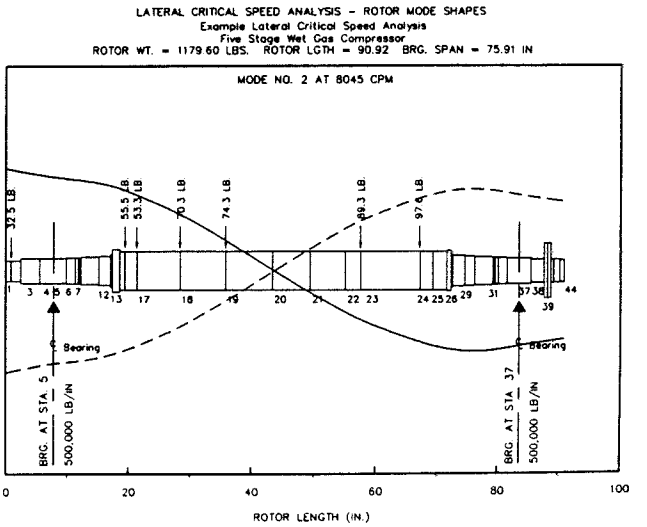

Figure 6. Undamped Mode Shape for Second Critical Speed.

stiffness and damping parameters. The critical speeds can shift considerably as a function of bearing tolerances.

- Understand the mode shape of the critical speed. The mode shapes are used to assess the response of the rotor to potential unbalances. For example, a rotor that has a conical whirl mode (second critical) would be sensitive to coupling unbalance, but not strongly influenced by midspan unbalance.

ROTOR RESPONSE TO UNBALANCE

The computer program discussed can calculate the elliptical shaft orbit at any location along the length of a rotor for various types of bearings, pedestal stiffnesses, pedestal masses, seals, labyrinths, unbalance combinations, etc. Such programs are used to determine the installed rotor's response to unbalance and accurately predict the critical speeds over the entire range of variables.

The anticipated range of rotor response should be calculated with the range of bearing values and various combinations of unbalance. This is important since one part of the API specifications 617 (2.9.3.1) [13] states:

> The actual critical speed responses, as revealed on the test stand with a rotor unbalance magnitude in accordance with 2.9.2.4, Item d, placed at a location (usually the coupling) determined by the vendor, shall be the criteria for confirming the validity of the damped unbalanced response analysis.
>
> Note: It is recognized that the dynamic response of the machine on the test stand will be a function of the agreed-upon test conditions and that unless the test stand results are obtained at the conditions of pressure, temperature, speed, and load expected in the field, they may not be the same as the results expected in the field.
>
> Paragraph 2.9.3.3 indicates that
>
> Additional testing and correction of the original damped unbalanced rotor response analysis will be required if, from the test data described above and/or a phase or amplitude indication in the damped unbalanced response analysis (based on the unbalance conditions described in 2.9.2.4, Item b), it appears that either of the following condition exists:
>
> (a) Any critical response will fail to meet the separation margin requirements (see 2.9.2.5) or will fall within the operating speed range.
>
> (b) The requirements of 2.9.2.6 have not been met.

The significance of this can be appreciated from the results of a balanced mechanical test and the unbalance sensitivity test for a centrifugal compressor (Figure 7). It can be seen that the balanced run data showed no troublesome resonances. When the out-of-phase sensitivity tests were made, high amplitude critical speeds were excited.

In the design stage, it is not possible to know the exact installed configuration with regard to bearings (clearance, preload) and balance (location of unbalance). Usually a mechanical test will be limited to one configuration (clearance, preload, unbalance) that may not show any problem. Changes introduced later by spare parts during turnarounds, for example, may change sensitive dimensions that may result in a higher response. For this reason, some satisfactorily operating machines change vibration characteristics after an overhaul.

The actual critical speed locations as determined from response peaks caused by unbalance are strongly influenced by the following factors [3, 8, 9, 10]:

- bearing direct stiffness and damping values

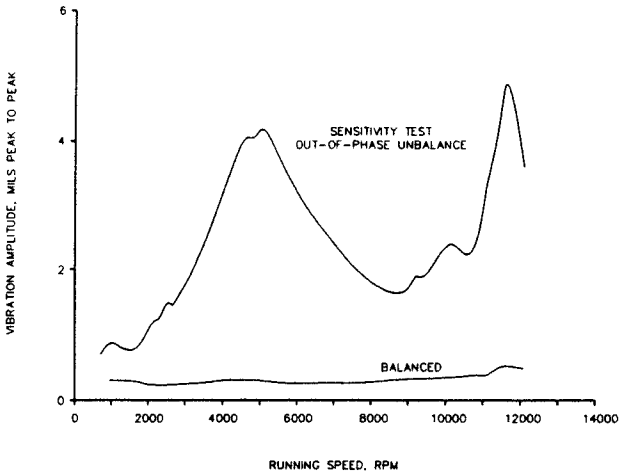

Figure 7. Comparison of Balanced Mechanical Run and Out-of-Phase Unbalance Sensitivity Test.

- bearing cross coupled stiffness and damping values
- location of the unbalance
- location of measurement point
- bearing support flexibility

To illustrate the sensitivity of the peak response critical speeds for the example compressor (whose critical speed map is given in Figure 3), the responses due to coupling unbalance and midspan impeller unbalance were calculated. The allowable vibration amplitude (based on API 617) for this compressor was 1.2 mil peak-to-peak, since its maximum continuous speed was 8500 rpm.

The API allowable unbalance used for the analysis is

$$UB = 4\,\frac{W}{N} \tag{5}$$

where:

UB = allowable unbalance, oz-in
W = rotor weight, lb
N = rotor speed, rpm

Usually rotor response to unbalance calculations are made for midspan unbalance, coupling unbalance, and moment type unbalance. An unbalance of 40 W_c/N (where W_c is the weight of the coupling) is usually applied at the coupling to excite the rotor. For moment unbalances, a weight is placed at the coupling, and another equal unbalance is placed out-of-phase on the impeller or wheel furthest from the coupling, or on the other coupling if it is a drive-through machine. This type of unbalance was used in the mechanical run sensitivity test shown in Figure 7.

Sensitivity To Bearing Clearance

The computer response analyses for coupling unbalance are given in Figure 8 for minimum, nominal, and maximum clearances. A critical speed response was predicted near 3800 cpm for the minimum clearance case. The predicted amplitudes at rated speed were less than the API limit for the minimum and nominal clearances. When the maximum bearing clearance was used, the responses became more pronounced and the predicted amplitudes at rated speed exceeded the API limit of 1.2 mil. The increased clearance lowered the predicted peak response to 8800 rpm, which is only 3.5 percent above the rated speed. This shows the sensitivity of a rotor to bearing clearance changes. For minimum or nominal bearing clearances, this rotor would meet

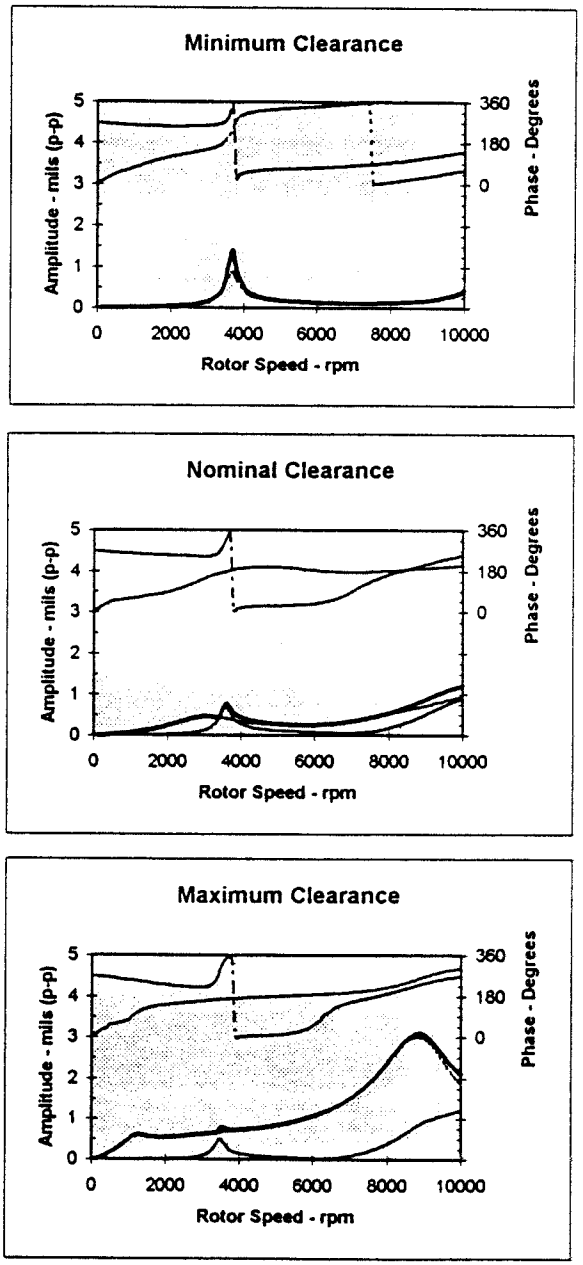

Figure 8. Calculated Unbalance Response for Range of Bearing Clearances.

the specifications. However, for maximum clearance bearings, it violates API 617.

It is often useful to consider the forced response mode shapes for understanding unbalance response. For example, the nominal bearing clearance case shown in Figure 8 showed two response peaks. The first is a well damped peak near 3000 rpm and the second is a sharper response near 3600 rpm. The forced response mode shapes for these two peaks are shown in Figures 9 and 10. They both are basically the first bending mode of the rotor. However, the lowest frequency mode responds mainly in the horizontal plane and is well damped, since there is motion at the bearings. The second peak is less damped because the amplitude at the bearings is lower. It is mainly a vertical mode. Three dimensional animation techniques are also useful for understanding these modes.

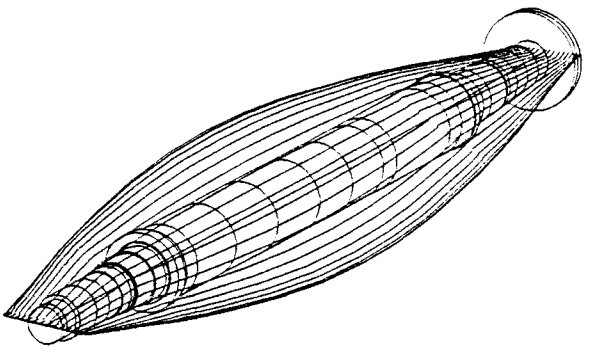

Figure 9. Mode Shape for Horizontal First Critical at 3000 RPM.

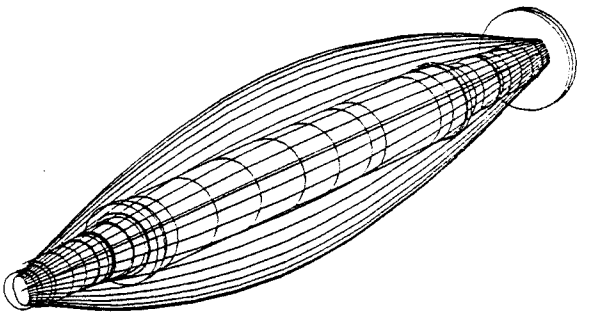

Figure 10. Mode Shape for Vertical First Critical at 3600 RPM.

Sensitivity to Unbalance Location

The influence of unbalance location on rotor response is illustrated by comparing the response calculations for midspan and coupling unbalances, as shown in Figure 11. The midspan unbalance excites the first mode near 3500 rpm. The response peak is well defined, with an amplification factor of about 14. The second mode is barely visible near 9100 rpm, with very low amplification.

For coupling unbalance, the first mode is de-emphasized, but the second mode is clearly identified at 8900 rpm with an amplification factor of about 5.5. This illustrates the importance of knowing the unbalance location when evaluating rotor response in the context of API or user company specifications.

Sensitivity to Pedestal and Foundation Flexibility

The stiffness, mass and damping of the bearing support structure should be considered in a rotordynamic audit. Basically, the bearing and pedestal stiffnesses combine as springs in series. If the bearing stiffnesses are very low compared to the pedestal stiffnesses, the critical speeds and rotor responses will not be greatly affected by the pedestal and support flexibility. Most rotordynamic computer programs can consider the pedestal mass, stiffness and damping values in the rotor response to unbalance calculations.

In the design stage, the determination of accurate values of stiffness/damping for the pedestal and supports can be difficult due to the complex shapes and uncertainties in the bolted joints, grout and other factors. Finite element programs can be used to determine the stiffness and damping values; however, this increases the cost and time of the analysis. For existing structures, the support flexibility can be experimentally determined and included in the rotordynamics calculations.

To determine if a complex finite element analysis of the support structure is needed, parametric runs can be made vary-

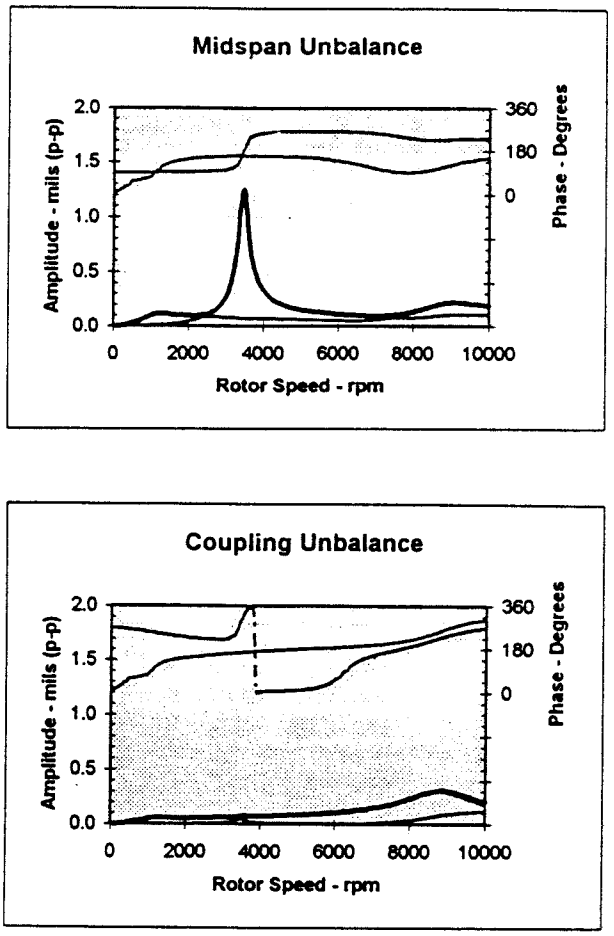

Figure 11. Comparison of Response for Midspan and Coupling Unbalance.

ing the support stiffness from large values to values comparable to the bearing stiffnesses. This information will show how sensitive the rotor critical speeds and responses are to pedestal stiffnesses. Generally, pedestal stiffnesses may vary from approximately 0.1 to 5.0 million lb/in. The horizontal stiffnesses are usually less than the vertical stiffnesses; therefore, the horizontal critical speeds will generally be lower than the vertical. Pedestal stiffnesses can be particularly important in the analysis of large rotors. For example, many induced draft fan systems have pedestal and foundation stiffnesses that are lower than typical bearing stiffnesses.

Liquid Pump Lateral Response Analyses

Pump rotordynamics are dependent on a greater number of design variables than are many other types of rotating equipment. Besides the journal bearing and shaft characteristics, the dynamic characteristics of the seals and the impeller-diffuser interaction can have significant effects on the critical speed location, rotor unbalance sensitivity, and rotorstability [4, 14, 15].

For modelling purposes, seals can be treated as bearings in the sense that direct and cross coupled stiffness and damping properties can be calculated based on the seal's hydrostatic and hydrodynamic properties. Seal clearances, geometry, pressure drop, fluid properties, inlet swirl, surface roughness and shaft speed are all important in these calculations. Since the pressure drop across seals increases approximately with the square of the pump speed, the seal stiffness also increases with the square of the speed. This increasing stiffness effect is often thought of as a "negative" mass effect, sometimes referred to as the "Lomakin effect" or the "Lomakin mass" [4]. In some cases, the theoretical Lomakin mass or stiffness effect can be of sufficient magnitude to prevent the critical speed of the rotor from ever being coincident with the synchronous speed.

The accurate prediction of the stiffness and damping properties of seals for different geometries and operating conditions is a subject of ongoing research. The basic theories presented by Black [16] have been modified to account for finite length seals, inlet swirl, surface roughness, and other important parameters. However, a universally accepted procedure to accurately predict seal properties is not available for all the types of seals in use today. This is particularly true for grooved seals. Unless seal effects are correctly modelled, calculated critical speeds can be significantly different from actual critical speeds.

A series of grooved seal designs used in commercial pumps has been tested by Childs [4], and techniques have been developed, whereby the seal geometry can be specified and the characteristics calculated for specific assumptions with regard to inlet swirl, groove design, etc.

The rotordynamic analysis of a ten-stage centrifugal pump using serrated (grooved) seals will be used to illustrate a design audit of a pump. The first step in a rotordynamic analysis of a pump is to model the basic rotor, using the lumped parameter techniques. A sketch of the rotor with the location of the seals and bearings is given in Figure 12. Note that the pump shaft is analyzed as a rotor with 14 bearings (two cylindrical bearings, 10 wear rings, the balance sleeve, and the center bushing).

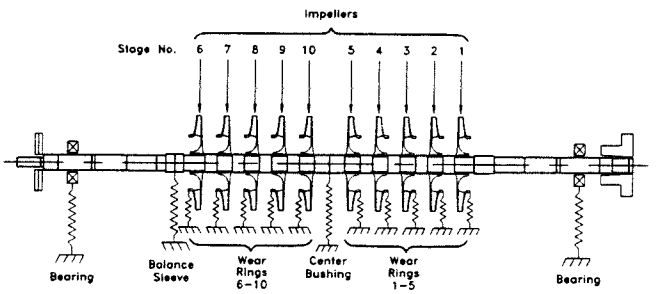

Figure 12. Pump Rotor Model Showing Locations of All Effective Bearings.

Rotor unbalance response calculations are the key analysis in the design stage for determining if a pump rotor is acceptable from a dynamics standpoint. In order to bracket the expected range of critical speeds, the unbalance response of a pump should be analyzed for three cases. The first case with no seal effects and maximum bearing clearances, which represents the overall minimum expected support stiffness for the rotor (lowest critical speed). The second case would be with minimum seal and bearing clearances that represents the maximum expected support stiffness and therefore, the highest critical speed. The third case should be considered with maximum bearing clearances and seal clearances of twice the design clearance to simulate worn seals which represents the pump condition after long periods of service.

The calculated critical speed for the 10 stage pump for the minimum bearing clearance, new seal case was 6000 cpm as shown in Figure 13(a). The American Petroleum Institute (API) Standard 610 allowable unbalance was applied at the rotor midspan to excite the first mode. The results of the intermediate (worn seals) case are presented in Figure 13(b). The worn seals reduce the predicted response peak to approximately 5500 cpm.

With maximum clearances at the bearings and seals, the frequency lowers to 4800 cpm, as shown in Figure 13(c). The pump rated speed was 5000 rpm. For the minimum clearance, new seal case, the 20 percent separation margin required by API specifications was satisfied. However, as the seals wear, the separation margin reduces to an unacceptable level. This again emphasizes the importance of considering the range of tolerance in critical parameters when evaluating a rotor design.

Gear Shaft Lateral Response Analysis

When performing a lateral critical speed analysis of a gear shaft, the effect of the transmitted torque must be considered in the bearing load analysis. API 613 (Special-Purpose Gear Units For Refinery Services, 1977) specifies that the critical speeds should not be less than 20 percent above the operating speed. The critical speeds at approximately 10 percent, 50 percent, and 100 percent load and maximum continuous speed should be considered in the calculations.

The relationship of the various forces is shown in Figure 14 acting on a gear shaft that has helical gear teeth. Since the bearing forces will depend upon the gear weight and the transmitted horsepower, calculations should be made over the range of 10 percent to 100 percent load. Calculations made for an audit of a gear are given in Table 4. The gear shafts used four lobed bearings and the bearings stiffnesses and damping changed considerably as the load changed (Table 5). To evaluate the changes in fixed-element bearing properties, rotor response to unbalance calculations must be made.

The effect of load variation for the rotor response can be seen in Figure 15, which shows the response to midspan unbalance for 10, 50 and 100 percent load. It can be seen that the critical speed would coincide with rated speed between 50 and 100 percent load.

It is often difficult, if not impossible, to meet the required separation margin of API 613 over the entire load range. Generally, the gear shaft and bearing designs are changed to move the critical speeds from the disallowed range for the normal loads. The response analysis is then made to verify that the vibrations will be below acceptable values, even if on resonance at the lower loads.

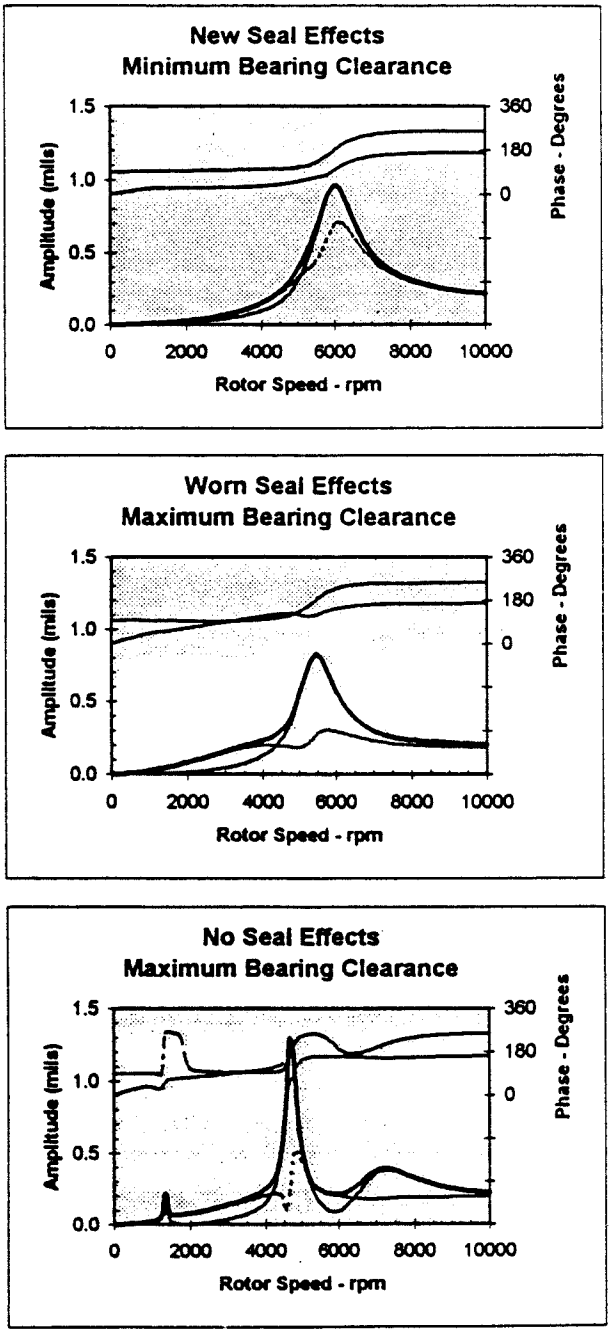

Figure 13. Response of Liquid Pump Rotor for Varying Seal and Bearing Clearances.

ROTOR STABILITY ANALYSIS

Rotor stability continues to be of major concern, especially for high pressure compressors [17, 18, 19, 20, 21, 22]. Rotor instability occurs when the rotor destabilizing forces are greater than the rotor stabilizing forces. The destabilizing forces can be caused by the bearings, oil seals, friction in shrink fits, etc. Aerodynamic loading effects such as rotating stall in either

Table 4. Bearing Loads as a Function of Transmitted Horsepower.

HORSEPOWER = 31046. BHP
DRIVER SPEED = 5670. RPM
DRIVEN SPEED = 10742. RPM
PD DRIVER = 23.190 INCHES
PD DRIVEN = 12.240 INCHES
PRESS. ANG. = 20. DEGREES
HELIX ANG. = 14. DEGREES
WEIGHT LOADS: A = -778.0 LBS MESH DIST: A = 14.17 IN.
B = -1349.0 LBS B = 14.17 IN.
C = -527.0 LBS C = 14.17 IN.
D = -396.0 LBS D = 14.17 IN.

RIGHT HANDED HELIX ON DRIVER
UPMESH - SPEED INCREASER

BULL GEAR (DRIVER) BEARING FORCES - LBS									
% LOAD	BRG	|Fsep|	|Ftan|	Fwt	Fxnet	Fynet	MAG	DEG	Fax
100.00	A	5568.	14875.	-778.	-2646.	-15653.	15875.	260.	7142.
100.00	B	5568.	14875.	-1349.	-8490.	-16224.	18311.	242.	
75.00	A	4176.	11156.	-778.	-1984.	-11934.	12098.	261.	5357.
75.00	B	4176.	11156.	-1349.	-6368.	-12505.	14033.	243.	
50.00	A	2784.	7438.	-778.	-1323.	-8216.	8321.	261.	3571.
50.00	B	2784.	7438.	-1349.	-4245.	-8787.	9758.	244.	
25.00	A	1392.	3719.	-778.	-661.	-4497.	4545.	262.	1786.
25.00	B	1392.	3719.	-1349.	-2123.	-5068.	5494.	247.	
10.00	A	557.	1488.	-778.	-265.	-2266.	2281.	263.	714.
10.00	B	557.	1488.	-1349.	-849.	-2837.	2961.	253.	
PINION (DRIVEN) BEARING FORCES - LBS									
% LOAD	BRG	|Fsep|	|Ftan|	Fwt	Fxnet	Fynet	MAG	DEG	Fax
100.00	C	5568.	14875.	-527.	7110.	14348.	16013.	64.	-7142.
100.00	D	5568.	14875.	-396.	4026.	14479.	15028.	74.	
75.00	C	4176.	11156.	-527.	5333.	10629.	11892.	63.	-5357.
75.00	D	4176.	11156.	-396.	3019.	10760.	11176.	74.	
50.00	C	2784.	7438.	-527.	3555.	6911.	7771.	63.	-3571.
50.00	D	2784.	7438.	-396.	2013.	7042.	7324.	74.	
25.00	C	1392.	3719.	-527.	1778.	3192.	3653.	61.	-1786.
25.00	D	1392.	3719.	-396.	1006.	3323.	3472.	73.	
10.00	C	557.	1488.	-527.	711.	961.	1195.	53.	-714.
10.00	D	557.	1488.	-396.	403.	1092.	1163.	70.	

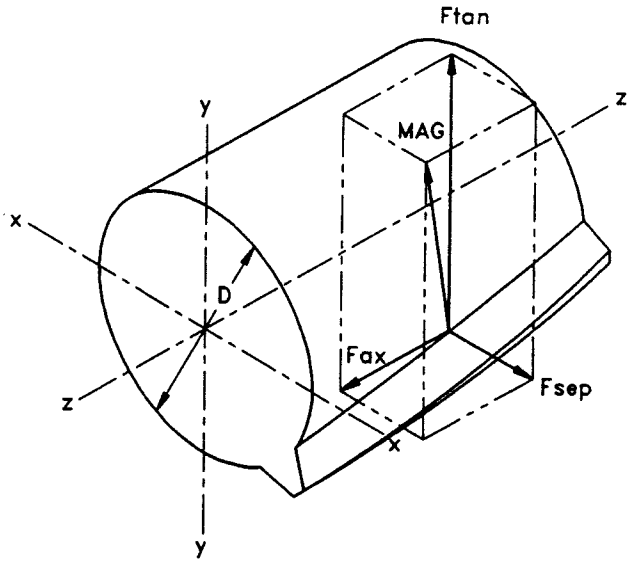

Figure 14. Transmitted Gear Load on Helical Gear Teeth.

Table 5. Hydrodynamic Bearing Coefficients for Four Lobed Bearing.

Low Speed Gear L/D = 0.867 D = 7.086 in. L = 6.14 in. CL = 6.03 mils (nominal) RPM = 5670								
% LOAD	Kxx $\times 10^6$	Kxy $\times 10^6$	Kyx $\times 10^6$	Kyy $\times 10^6$	Cxx	Cxy	Cyx	Cyy
10	0.075	0.564	−1.110	1.080	1870	361	315	3780
50	1.040	0.559	−3.460	5.130	2360	−322	297	12000
100	2.500	0.972	−7.760	12.400	3880	−1960	−1890	28900
High Speed Pinion L/D = 1 D = 6.75 in. L = 6.75 in. CL = 5.38 mils (nominal) RPM = 10742								
% LOAD	Kxx $\times 10^6$	Kxy $\times 10^6$	Kyx $\times 10^6$	Kyy $\times 10^6$	Cxx	Cxy	Cyx	Cyy
10	0.464	−0.175	0.708	0.976	656	14	422	1720
50	2.090	1.440	3.410	7.310	868	811	2250	8960
100	5.390	5.090	9.190	19.600	1256	2569	4859	24270

impellers or diffusers, impeller blade loading edge incidence, jets and wakes at impeller tips, diffuser stall, pressure pulsations and acoustical resonances, surge, and labyrinth seals also contribute destabilizing effects.

Instabilities in rotors can cause high vibrations with several different characteristics. They generally can be classified as bearing related, self-excited, and forced nonsynchronous instabilities. Oil whirl and half-speed whirl are bearing related instabilities and are caused by the cross coupling from the bearing oil film in fixed geometry bearings. Half speed whirl will result in rotor vibrations at approximately one-half of the running speed frequency. Oil whip describes a special type of subsynchronous vibration that tracks approximately half-speed up to the point where the speed is two times the first critical. As the speed increases, the subsynchronous vibration will remain near the first critical speed. These types of instabilities can generally be solved by changing the bearing design to a pressure dam, elliptical, offset-half bearing, or tilting pad bearing.

A second type of instability can occur on any rotor, including those with tilted pad bearings. The vibrations will usually occur near the rotor first critical speed or may track running speed at some fractional speed. These types of instability vibrations are sometimes referred to as self-excited vibrations, since the motion of the rotor creates the forcing mechanism that causes the instability [10].

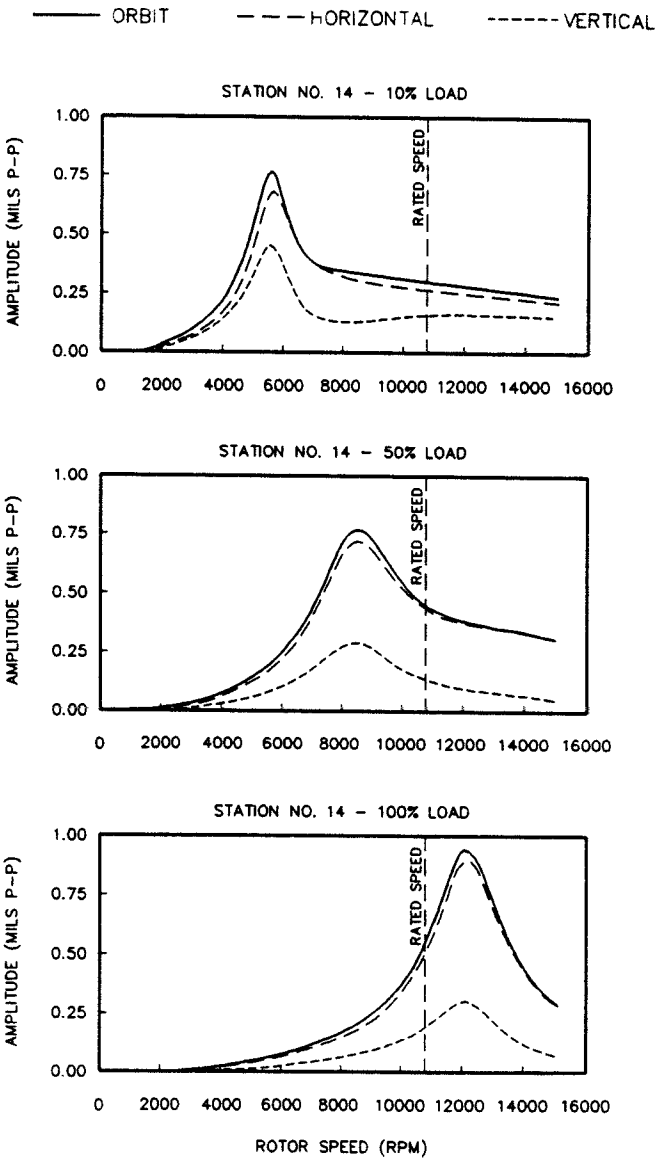

Figure 15. Calculated Pinion Gear Response for 10%, 50% and 100% Load with Midspan Unbalance.

A third type of instability is called a forced nonsynchronous instability and can be caused by stage stall in the last stages of the compressor, or by acoustical resonances in the system [21, 22]. This type of instability usually occurs at 10 to 20 percent of running speed as dictated by the acoustical response characteristics of the diffuser and passage geometry.

The predominant method used in performing a stability analysis is to calculate the damped (complex) eigenvalues and logarithmic decrement (log dec) of rotor, bearing, and seal assembly. A positive log dec indicates that a rotor system is stable, whereas a negative log dec indicates an unstable system. Experience has shown that due to uncertainties in the calculations, the calculated log dec should be greater than 0.1 when all destabilizing effects have been considered to ensure stability. Damped eigenvalues generally occur near the shaft critical speeds; however, in some heavily damped rotors they can be significantly different from the responses due to unbalance. In the past, some difficulties were encountered when using the transfer matrix solution techniques for the solution of the insta-

bility frequencies since some of the roots could be missed, as discussed by Vance [9]. Using the matrix based eigenvalue solution method, no roots are missed.

Rotor stability programs are available that can model the rotor stability for most of the destabilizing mechanisms; however, some of the mechanisms that influence it are not clearly understood. It has been well documented that increased horsepower, speed, discharge pressure, molecular weight, and pressure ratio can cause a decrease in the rotor stability. Many units that are stable at low speeds and pressure become unstable at higher values. To predict the stability of a rotor at the design operating conditions, the rotor shaft, bearings, and seals are modelled and the log dec is calculated as a function of aerodynamic loading. An equation, based on experience from several instability problems, includes many of the factors which have shown to be important in rotor stability, such as horsepower, speed, diameter of impeller, density ratio across the compressor, impeller, and diffuser restrictive dimensions, and molecular weight of fluid was published by Wachel [18]. This equation can be used to predict the approximate aerodynamic loading that exists. The aerodynamic loading is a cross coupling term, usually distributed at the impellers. Conceptually, it can be thought of as a component which detracts from the stabilizing forces in the system.

$$K_{yx} = \frac{6300\ HP\ MW}{D\ N\ h}\ \frac{\rho_d}{\rho_s} \qquad (6)$$

where: K_{yx} = aerodynamic loading, lb/in
HP = horsepower
MW = molecular weight of fluid
ρ_d = discharge density of fluid, lbs/in^3
ρ_s = suction density of fluid, lbs/in^3
D = impeller tip diameter, in
N = speed, rpm
h = resistive dimension in flow path, in (usually impeller tip width or diffuser width)

In using this equation, the most conservative approach is to use the last stage dimensions to calculate the aerodynamic loading, assuming the entire horsepower is absorbed on that stage. The aerodynamic loading can then be equally distributed over the impellers in the stability analysis. If the needed information is available on all the impellers, the aerodynamic loading can be calculated stage by stage and applied at the appropriate impeller in the stability analysis.

It is recognized that, in some machines, some additional direct stiffness occurs from the aerodynamic loading and many times the measured instability frequency will be slightly higher than the calculated frequency, assuming no direct stiffness effects.

In the normal audit procedures, the stability is calculated as a function of aerodynamic loading with a computer model of the rotor, bearings, and seals. In the evaluation of the stability, it is desirable to have a log dec at zero aerodynamic loading greater than 0.3 and still greater than 0.1 at the calculated aerodynamic loading. The log dec should be calculated for the range of bearing and seal properties expected as shown in Figure 16. This is a plot for the lowest forward whirl mode and indicates the estimated aerodynamic loading. Note that this rotor is predicted to be stable for nominal to maximum clearance bearings, but unstable for minimum clearance bearings.

Kirk [22] has presented a stability criteria that uses the discharge pressure times the differential pressure across the

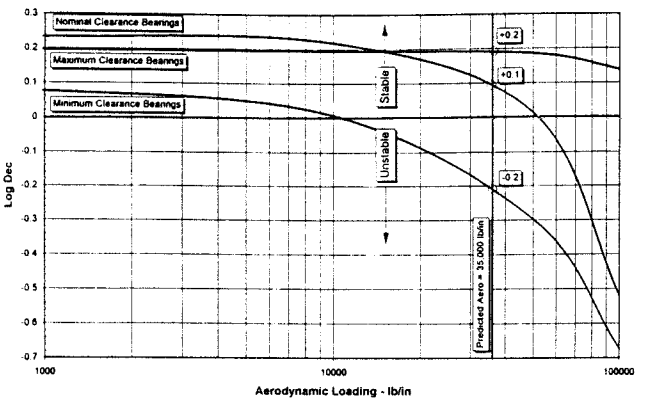

Figure 16. Calculated Logarithmic Decrement vs *Aerodynamic Loading for Range of Bearing Clearances.*

machine *vs* the ratio of running speed to the first critical speed. Stroh [23] suggested a work/energy relationship to determine the aerodynamic loading. Atkins and Perez [24] have presented methods to test rotors to define their stability limits. Several studies have found that instabilities can be controlled through the use of honeycomb seals [25, 26].

TORSIONAL CRITICAL SPEED ANALYSES

All rotating machinery systems experience torsional oscillations to some degree during startup, shutdown, and continuous operation. Severe torsional vibrations often occur with the only indication of a problem being gear noise or coupling wear. Excessive torsional vibrations can result in gear wear, gear tooth failures, key failures, shrink fit slippage, and broken shafts in severe cases [27, 28].

The severity of torsional oscillations and stress depends upon the separation margin between the excitation frequencies from the machinery and the torsional natural frequencies. The magnitude of the stress also depends upon the amplification factor(damping) and the stress concentration factors.

The API codes for turbines, compressors, and pumps (611, 617, 610) specify that the torsional natural frequencies of the system be at least 10 percent below any operating speed or at least 10 percent above the trip speed. In some systems, multiples of operating speed and blade passing frequencies can excite torsional natural frequencies. An additional margin of at least five percent should be allowed for calculation inaccuracy in torsional analyses. Variable frequency drive motors typically operate from 20 to 100 percent of the motor design speed, making it virtually impossible to meet the separation margin requirements throughout the speed range. Other types of drivers with wide speed ranges may have similar problems.

An independent torsional analysis can be performed to determine if the operating stresses are below the endurance limit stress for the shaft material. A detailed torsional analysis would include the following items:

- Calculation of the system torsional natural frequencies and mode shapes.
- Development of an interference diagram which shows the torsional natural frequencies and the excitation frequencies as a function of speed.
- Calculation of the dynamic torsional stresses in all the shafts in the system, based on the expected dynamic torque modulations, stress concentration factors, and amplification factors.
- Calculation of the coupling torques to ensure that the couplings can withstand the dynamic load torques.

• Comparison of the calculated results with applicable codes or specifications to determine compliance with regard to separation margin, stresses, gear loading, and coupling dynamic torque.

• Calculation of transient torsional stresses and number of allowable startups for systems with synchronous motor drives and variable frequency drives.

• Calculation of allowable number of electrical faults, line-to-line short circuits, and three phase short circuits.

Torsional natural frequencies are a function of the torsional masses and the torsional stiffnesses between the masses. The natural frequencies and mode shapes can be calculated by Holzer or eigenvalue-eigenvector methods (modal superposition). The eigenvalue-eigenvector method for calculating the torsional natural frequencies and mode shapes is used most often today, since it can easily calculate the forced vibration response of systems due to various forcing functions at different mass locations. This method can also include the phasing of all excitation torques, which is more difficult to do with the Holzer method.

An example of a mass-elastic diagram of a torsional system is give in Figure 17. The natural frequencies and mode shapes associated with the first four natural frequencies are given in Figure 18. The mode shapes can be used to determine the most influential springs and masses in the system. This information is important if encroachment is calculated and system changes must be made to detune the systems. Parametric analyses should be made of the coupling stiffness if changes are necessary, since many torsional problems can be solved by coupling changes.

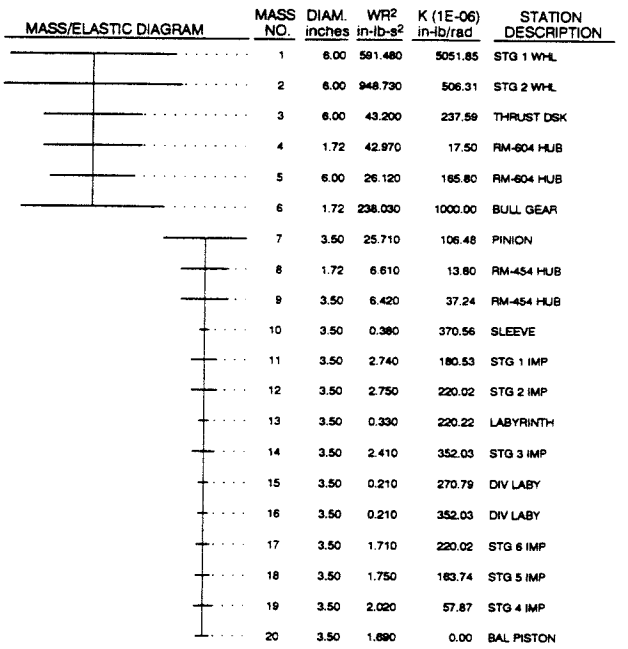

MASS NO.	DIAM. inches	WR² in-lb-s²	K (1E-06) in-lb/rad	STATION DESCRIPTION
1	6.00	591.480	5051.85	STG 1 WHL
2	6.00	948.730	506.31	STG 2 WHL
3	6.00	43.200	237.59	THRUST DSK
4	1.72	42.970	17.50	RM-604 HUB
5	6.00	26.120	165.80	RM-604 HUB
6	1.72	238.030	1000.00	BULL GEAR
7	3.50	25.710	106.48	PINION
8	1.72	6.610	13.80	RM-454 HUB
9	3.50	6.420	37.24	RM-454 HUB
10	3.50	0.380	370.56	SLEEVE
11	3.50	2.740	180.53	STG 1 IMP
12	3.50	2.750	220.02	STG 2 IMP
13	3.50	0.330	220.22	LABYRINTH
14	3.50	2.410	352.03	STG 3 IMP
15	3.50	0.210	270.79	DIV LABY
16	3.50	0.210	352.03	DIV LABY
17	3.50	1.710	220.02	STG 6 IMP
18	3.50	1.750	163.74	STG 5 IMP
19	3.50	2.020	57.87	STG 4 IMP
20	3.50	1.690	0.00	BAL PISTON

Figure 17. Torsional Mass-Elastic Data for Gas Turbine-Compressor or Train.

An interference diagram for the turbine-driven compressor with a gear box is given in Figure 19. The rated speeds are 6250 rpm for the gas turbine and 11,875 rpm for the compressor. In this system, excitation at 1× and 2× the gas turbine and compressor speeds are possible. The 1× excitation of gas turbine speed excites the first critical speed at 1907 rpm; however, the rated speed is within 10 percent of the calculated second natural frequency at 6869 rpm.

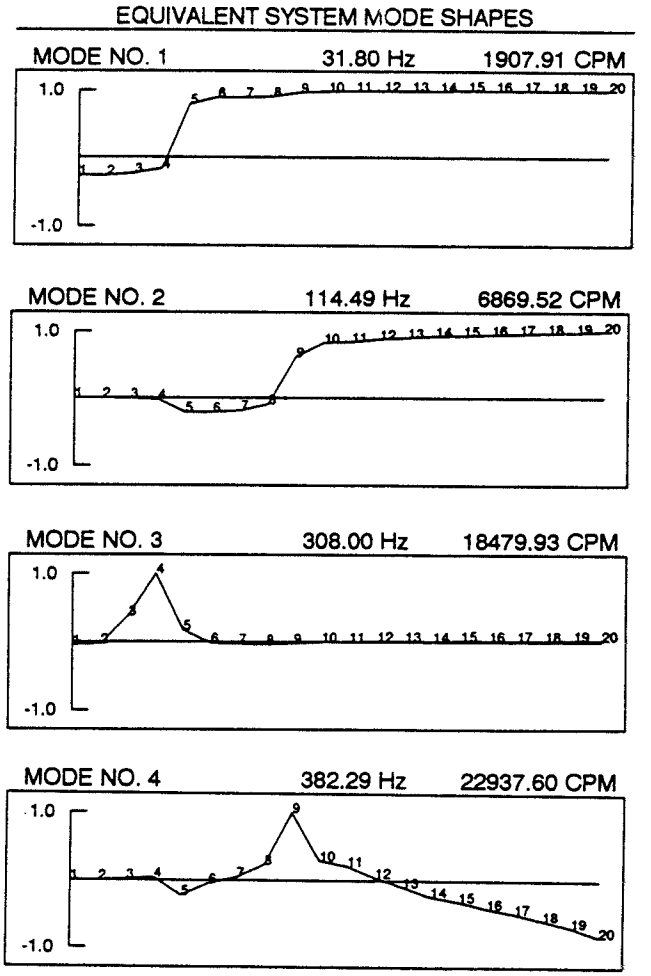

Figure 18. Torsional Natural Frequencies and Mode Shapes.

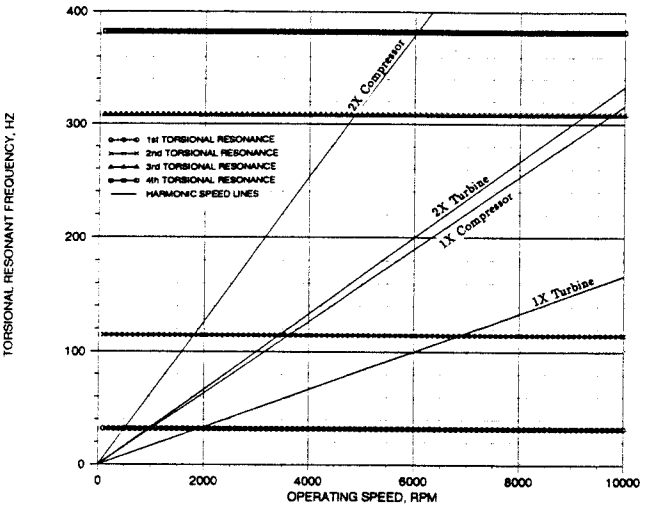

Figure 19. Interference Diagram for Gas Turbine-Compressor Train.

For the example problem, the stresses calculated *vs* speed (Figure 20) show that the stresses from excitation at the bull gear would be acceptable at the maximum speed; however, if the trip speed is near the torsional natural frequency at 6869 rpm, the stresses would be excessive. The summary of the stress calculations at the second natural frequency is given in Table 6. It shows

Table 6. Torsional Stress Calculations at the Second Torsional Natural Frequency for One Percent Excitation at the Bull Gear.

Maximum Resultant Torsional Stresses at 6869 RPM					
Shaft	SCF	Stress kPa 0–p		Stress psi 0–p	
		No SCF	w/SCF	No SCF	w/SCF
1	2.0	166	332	24	48
2	1.5	416	624	60	90
3	3.0	408	1225	59	178
4	*Dynamic Torque 252 N-m (2230 in-lbs)*				
5	3.0	66	199	10	29
6	*Dynamic Torque 1926 N-m (17049 in-lbs)*				
7	3.0	9881	29644	1433	4299
8	*Dynamic Torque 1411 N-m (12486 in-lbs)*				
9	3.0	8088	24264	1173	3519
10	1.5	7919	11879	1149	1723
11	1.5	6672	10008	968	1451
12	1.5	5367	8051	778	1168
13	1.5	5206	7810	755	1133
14	1.5	4003	6005	581	871
15	1.5	3897	5846	565	848
16	1.5	3789	5684	550	824
17	1.5	2903	4355	421	632
18	1.5	1985	2977	288	432
19	1.5	912	1367	132	198

that a one percent torque excitation on the bull gear would cause a maximum torsional stress of 3519 psi zero to peak in shaft 9, which is the compressor shaft between the coupling and the first sleeve. The dynamic torque modulation across the couplings are calculated for the applied input modulation by using an effective diameter of 1.72. For this mode, the maximum torsional vibrations occur across the compressor coupling and the dynamic torque modulation was 12486 in-lb. The compressor speed (1×) excitation would excite the first torsional natural frequency at 1005 rpm and the second natural frequency at 3619 rpm on the gas turbine.

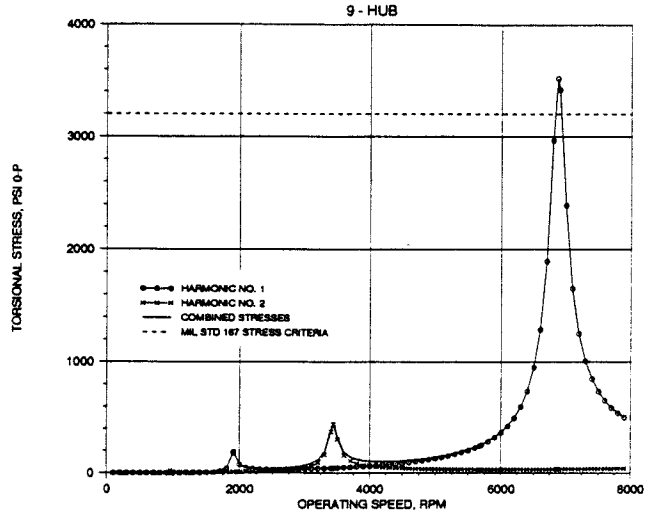

Figure 20. Calculated Torsional Stresses for Excitation at Bull Gear.

Steady State Torque Excitation

Based on experience, the magnitude and most likely frequencies of the torque excitations that should be used in the torsional design audit are given by Wachel and Szenasi [27] in Table 7 and discussed below. Since the magnitude of the torsional excitations are based on empirical data, the values should be used with caution and verified by field test measurements for critical systems.

Table 7. Steady State Torsional Excitation Sources.

Source	Frequency	Amplitude % T_{SS} 0–p	Comments
Centrifugal Compressors Turbines	1× 2×	1.0% $\frac{1}{2}$	Misalignment
Pumps, Fans	B×, β × B = Number of Impeller Vanes β = Number of Diffuser Vanes	$\left(\frac{1}{B}\right)$% $\frac{1}{\beta}$%	Assumes No Acoustical Resonances
Gears	1× 2×, 3×, n×	1% $\frac{1}{2}, \frac{1}{3}, \frac{1}{n}$ ...%	Worn Gears, Bad Allignment
Reciprocating Compressors, Pumps	1×, 2×, n×	TEC * [1-3]	*Torque Effort Curve (TEC) Must Be Developed for Each Cylinder
Lobed Blowers	1×, 2×, n×	10-40% Typical	Harmonic Torques Depend Upon Number of Lobes and Their Timing
Engines (2 Cycle)	1×, 2× ... n×	Harmonic Torque Coefficients [1-3]	Based on Pressure - Time Wave From Power Cylinder Function of Mean Effective Pressure
Engines (4 Cycle)	$\frac{1}{2}$×, 1×, $1\frac{1}{2}$×, 2× $2\frac{1}{2}$× ... n×	Harmonic Torque Coefficients [1-3]	Based on Pressure - Time Wave From Power Cylinder Function of Mean Effective Pressure
Variable Frequency Motors	1×, 2× ... n× 6×, 12× ... 6n×	Mfg. Supplied	Depends Upon Type of VFD

- Power cylinders of reciprocating engines have excitation torques that are a function of the type of engine (two or four cycle, diesel or spark ignition) and the mean effective pressure for the cylinder.

- Reciprocating compressors and pumps can generate multiple harmonic torques that are a function of the compressor/pump loading condition, the physical geometry of the cylinder, the crankshaft geometry and the thermophysical properties of the gas or liquid.

- Gears of good quality usually generate dynamic torques with less than one percent zero—peak of the transmitted torque at one times (1×) running speed; however, larger percentages have been measured on worn gear sets and bevel gears.

- Centrifugal machinery torsional excitation at the running speed is generally less than one percent zero to peak of the steady-state torque. Torsional excitation from blade or vane passing frequency rarely exceeds 1/(number of blades) percent zero to peak of the steady load torque unless amplified by acoustic interaction. Again, these assumed excitations are based on experience and may have to be verified for critical applications.

- Couplings that are misaligned or eccentric can produce a torque fluctuation, particularly if some backlash occurs in gear couplings. The frequency of excitation will be a multiple of operating speed, generally at one and two times. This is similar to the excitation developed by a universal joint that can produce a high second order excitation. A gear coupling can also produce a low level, high frequency, torsional excitation.

- Three phase motors should not have a net dynamic torque component at the electrical frequency; however, pulsating torques at motor speed have been documented in torsional tests. While operating at rated speed, motors can produce a fluctuating torque, if nonsymmetries exist such as unequal air gaps or

unbalanced current in the armature or field. In the calculation procedure, a value of 1.0 percent zero to peak has been assumed for 1× electrical frequency (0.5 percent for 2×), and is considered conservative for most large HP industrial motors.

- Pulsations within process piping can be produced by the machine (running speed, blade passing frequency) or by the fluid flow excitation (Strouhal) and can react on the impeller or wheel to cause dynamic torques on the shaft system [29].

Steady State Stress Allowable

The torsional adequacy of the system should be evaluated by comparing the calculated torsional stresses in the shafts to the allowable endurance of the shaft material. Experience with many systems that have been analyzed and tested has shown US MIL STD 167 to be the easiest to apply and has been found to be conservative for most systems and is used by the authors. The calculated shaft shear stresses are considered acceptable when they are less than the ultimate tensile stress divided by 25, which is the value given for the shear endurance limit by US MIL STD 167. In critical shafting systems, a fatigue limit for the specific steel and heat treatment should be used to generate results with a higher confidence level. For example, extensive testing has been performed on engine crankshafts and criteria have been developed in terms of the combined stresses.

When comparing calculated stresses to this value, the appropriate stress concentration factor and a safety factor must be used. Generally, a safety factor of 2.0 is used for fatigue analysis and a typical stress concentration factor for a key way is 3.0 (USA Standard ANSI B17.1). Based on these values, a typical torsional stress allowable stress amplitude (zero to peak) thus becomes the ultimate tensile strength divided by 75, since the safety factor of 2.0 is included in the Mil Standard Value.

Transient Torsional Analysis

After the steady state torsional analysis is made, a transient torsional analysis should be made to evaluate the startup stresses and allowable number of startups for systems that experience transient events, such as synchronous motor system startups, variable frequency drive systems and systems that could experience electrical faults, such as short circuits (line-to-line and three phase) [27].

The transient analysis refers to conditions which continually cause fluctuations in the dynamic torque. The types of transient excitation torques that should be considered in a design audit are discussed later.

Synchronous Motors

Synchronous motors develop a strong oscillating torque during starting because of slippage between the rotor and stator fields. As the motor increases in speed, the torsional excitation frequency decreases from twice power line frequency (typically 120 Hz) linearly with speed toward zero. During this startup, the torsional system will be excited at several of its resonant frequencies if they are between 0 and 120 Hz, as shown in Figure 21 [27]. The response amplitudes and shaft stresses depend upon the resonant frequencies, the average and pulsating torque when the system passes through these resonant frequencies, the damping in the system, and the load torques. The startup analyses can be made for loaded or unloaded operation. The transient response is also affected by the starting acceleration rate of the motor. For slow motor startups, the system will stay at a resonant frequency for a longer period of time, allowing stresses to be amplified. If acceleration is rapid, passing through the resonance quickly will minimize the amplitude increase at resonant frequencies.

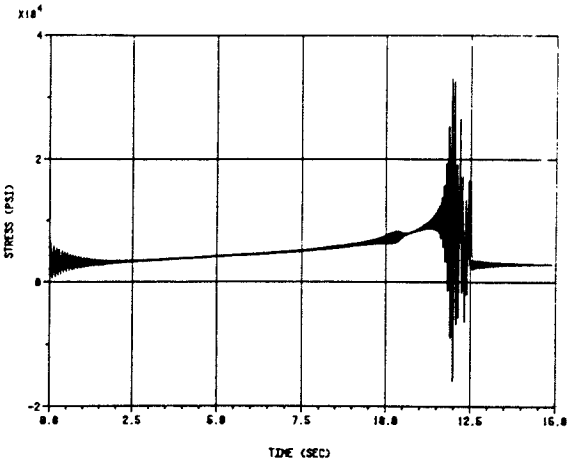

Figure 21. Torsional Stresses in Motor Shaft During Synchronous Motor Startup.

The pulsating torque can be strong enough to cause the torsional stresses to exceed the torsional endurance limit of the shaft. For this reason, the transient stresses must be calculated and compared to the endurance limit stress using cumulative stress criteria. It is not necessary that the transient stresses be less than the endurance limit stress; however, the stresses must be sufficiently low to allow an acceptable number of starts.

Electrical Faults

Electrical faults can produce braking torques several times the rated torque of the motor. Electrical faults are commonly analyzed for synchronous motors; however, they can occur in any motor or generator.

Variable Frequency Drive Systems

Variable frequency drive systems used with induction motors can generate high torque modulations at several multiples. Variable frequency controllers produce harmonic torques at multiples of 6 times the electrical frequency; however, the amplitude of the dynamic torques vary widely, depending upon the characteristics of each type of drive, and the manufacturer's design details [27]. The most common types used for large horsepower induction motors are discussed below:

- Voltage source inverter (VSI)—The inverter switches the voltage to produce a stepped waveform. At low frequency operation the current follows the stepped shape of the voltage waveform, but in the mid-frequency and high-frequency range the current waveform approaches a sinusoid and reasonable smooth motor speed is achieved.

- Current source inverter (CSI)—The inverter switches the current to produce a stepped waveform which, with a greater number of steps, approaches a sinusoid. The stepped waveform results in torque harmonics at multiples of the number of steps.

- Pulse width modulation (PWM)—High speed switching of the voltage is done to produce a basically sinusoidal current waveform with harmonics only related to the high frequency of the voltage pulses.

- Load commutated inverter (LCI)—This is used with synchronous motors and is similar to the CSI system; however, the circuitry is simpler and, hence, more reliable.

An interference diagram for one such variable drive system is given in Figure 22. It is difficult to remove all coincidence of resonances with the excitation sources over a wide speed range; therefore, stress calculations must be made to evaluate the

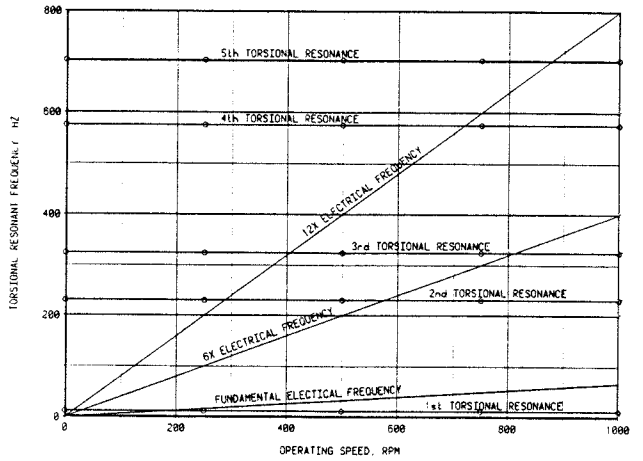

Figure 22. Interference Diagram for Induction Motor with Variable Speed Drive.

adequacy of the system stresses on each of the resonances. When variable speed drive systems are used with reciprocating compressors, it is difficult to avoid the excitation of one of the torsional resonances (Figure 23).

Cumulative Fatigue Stress Analysis

Since stresses occurring during startups and electrical faults are transient, they should be evaluated on the basis of cumulative fatigue if they exceed the endurance limit. Cumulative fatigue analysis is used to estimate how many cycles of a certain stress level may be endured before shaft failure would occur. The analysis determines the amount of fatigue incurred by each shaft during one startup as a result of stresses in excess of the shear endurance limit. The number of allowable startups can then be determined. In a variable frequency drive system, load variations can also result in a significant change in the transmitted torque, which constitutes a stress reversal. For instance, changing from full load to minimum load and then back to full load represents a stress reversal that may exceed the shear endurance limit, particularly if stress concentrations are present.

Many different fatigue analysis techniques are available for calculating cumulative fatigue damage. The major differences usually appear in the S-N curves, fatigue reduction factors, and stress range counting methods.

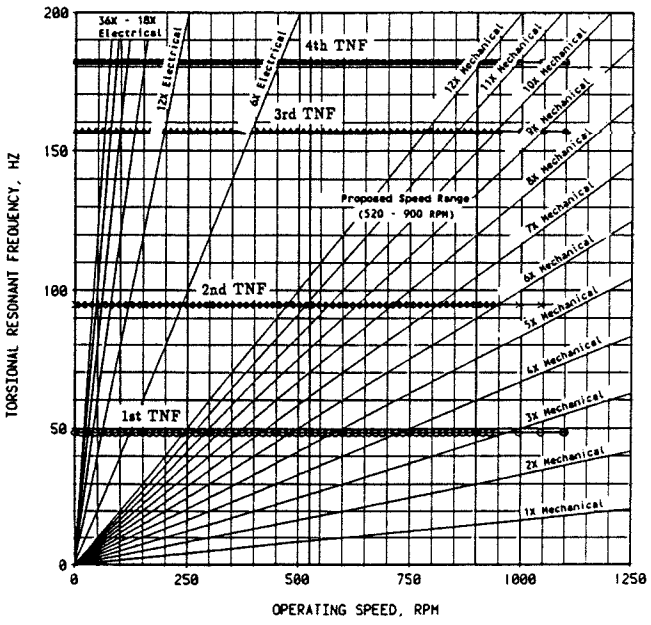

Figure 23. Interference Diagram for Variable Frequency Drive System with Reciprocating Compressor.

IMPELLER AND BLADE RESPONSES

A design audit should also include an assessment of the potential excitation of blade or impeller natural frequencies. Several papers have been presented at past Turbomachinery Symposiums that document such problems [30, 31, 32]. The impeller and blade response analysis should include:

- The blade and impeller natural frequencies
- The mode shapes
- Interference diagram indicating potential excitation mechanisms and the natural frequencies.

The interference diagram that gives the blade and impeller natural frequencies and the various potential excitation mechanisms is the key to prevention of failures. The resonances should be sufficiently removed from the major excitations in the operating speed range.

In the design stage, it is possible to calculate the natural frequencies and mode shapes using finite element method [FEM] computer programs that are available. However, the accuracy of predictions depends to a great extent upon the experience of the analyst and the complexity of the system.

Since the blades and impellers will usually be available in advance of the rotor assembly, the most accurate natural frequency and mode shape data can be obtained from shaker tests or by modal analysis methods. The modal analysis techniques use a two channel analyzer and an impact hammer and accelerometer to determine the natural frequencies and mode shapes. For example, the natural frequencies and mode shapes of a centrifugal impeller were measured using modal analysis techniques (Figure 24). When these frequencies were compared to values determined from a shaker study, good correlation was obtained. The mode shape for the 2.0 diameter mode is given in Figure 25.

An interference diagram for this impeller is given in Figure 26. Note that potential excitation mechanisms include vane passage frequency (15×) and 2 × vane passage frequency (30×).

It is sometimes impossible to completely avoid all interferences over a wide speed range, since there are so many natural frequencies. For most systems, in order for a failure to occur,

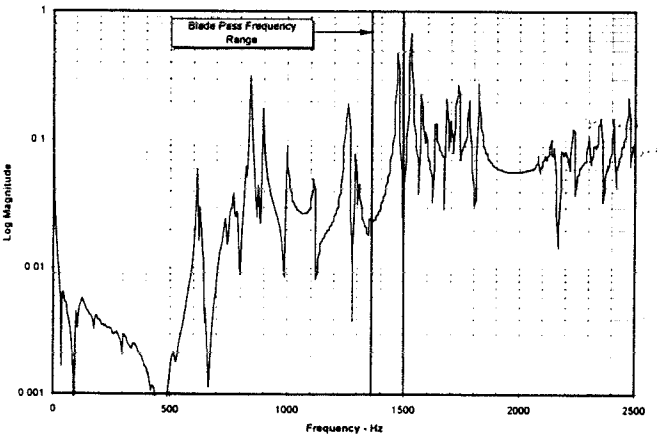

Figure 24. Frequency Response Function of Centrifugal Impeller.

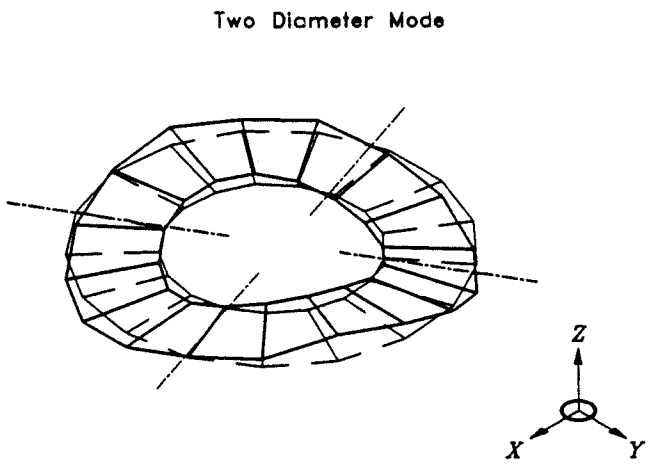

Figure 25. Two Diameter Mode Shape for Centrifugal Impeller Determined by Modal Analysis Tests.

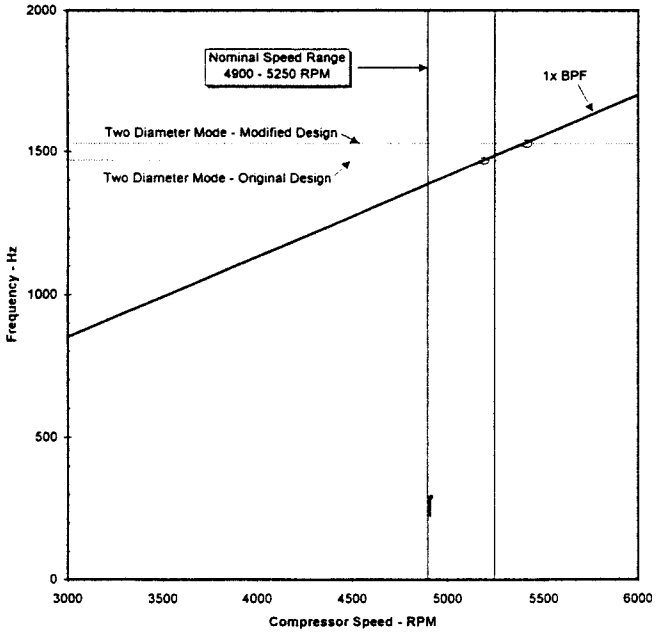

Figure 26. Interference Diagram for Centrifugal Impeller.

several things usually occur together. First, there must be a mechanical natural frequency. Second, there must be a definite excitation frequency, such as vane passing or diffuser vane frequency. Third, there must be some acoustical resonant frequency which amplifies the energy generated; and fourth, there must be the appropriate phase relationship that causes the pulsation to cause a shaking force on the impeller or blade. The best way to avoid such problems is to avoid coincidence of the resonances with the excitation mechanisms.

CONCLUSIONS

Typical rotordynamic design analyses have been presented along with some guidelines for determining the need and interpreting the results. It is difficult to determine when an audit is needed; however, it must be thought of as additional insurance that the machinery will run without major problems. Many of the analysis procedures and computer programs that have been developed are being used by both the manufacturer and by consultants who offer these design audit services. As with many computer programs, the interpretation of the computer results is dependent upon the skill and experience of the analyst. The manufacturer produces many machines that have no problems and, thus, has the confidence that the machinery will run successfully. The independent consultant usually is asked to look at machinery with some kind of problem or investigate a possible problem. Therefore, consultants probably look at the analysis from a slightly different viewpoint. The goal of the manufacturer, the user and the independent consultant is the same: everyone wants a trouble-free machine.

The independent audit generally takes place after the manufacturer has finalized drawings. In many cases where problems were found during the audit, it turned out that after the original analysis was made in the initial stages, some dimensions were changed causing significant changes in the calculated responses. If the independent audit is made, design problems can be resolved before installation.

Guidelines as to when an independent audit should be obtained, thus, are dependent upon many factors. Generally audits should be performed on:

- New or prototype machines that are extrapolations in horsepower, pressure, number of impellers, bearing span, or new concepts.
- Machines that, if unreliable, would cause costly downtime.
- Machines that are not spared (no backups).
- Expensive machines and installations where the cost of the audit is insignificant compared to the total project cost.

REFERENCES

1. Cook, C. P., "Shop *vs* Field Corrections to Equipment," *Proceedings of the Fourteenth Turbomachinery Symposium*, The Turbomachinery Laboratory, Texas A&M University, College Station, Texas (1985).
2. Bloch, H. P., *Improving Machinery Reliability, Practical Machinery Management for Process Plants, 1*, Houston, Texas: Gulf Publishing Company, Houston, Texas (1982).
3. Wachel, J. C., "Design Audits," *Proceedings of the Fifteenth Turbomachinery Symposium*, The Turbomachinery Laboratory, Texas A&M University, College Station, Texas (1986).
4. Childs, D. W., *Turbomachinery Rotordynamics Phenomena, Modeling, and Analysis*, New York, New York: John Wiley & Sons, Inc. (1993).
5. Crandall, S. H., "Rotordynamic Software," Rotating Machinery Dynamics, Proceedings of the Third International Symposium of Transport Phenomena and Dynamics of Rotating Machinery (ISROMAC-3), Washington D.C.: Hemisphere Publishing Corp., Washington, D.C., pp. 3-21 (1992).
6. Nicholas, J. C., "Tilting Pad Bearing Design," *Proceedings of the Twenty-Third Turbomachinery Symposium*, The Turbomachinery Laboratory, Texas A&M University, College Station, Texas (1994).
7. Allaire, P. E. and Flack, R. D., "Design of Journal Bearings for Rotating Machinery," *Proceedings of the Tenth Turbomachinery Symposium*, The Turbomachinery Laboratory, Texas A&M University, College Station, Texas (1981).
8. Zeidan, Fouad Y. and Paquette, Donald J., "Application of High Speed and High Performance Fluid Film Bearings in Rotating Machinery," *Proceedings of the Twenty Third Turbomachinery Symposium*, The Turbomachinery Laboratory, Texas A&M University, College Station, Texas (1994).

9. Vance, J. M., *Rotordynamics of Turbomachinery*, New York, New York: John Wiley & Sons, Inc. (1988).
10. Ehrich, F. F., *Handbook of Rotordynamics*, New York, New York: McGraw-Hill, Inc. (1992).
11. Kirk, R. G., "Oil Seal Dynamics: Consideration for Analysis of Centrifugal Compressors," *Proceedings of the Fifteenth Turbomachinery Symposium*, The Turbomachinery Laboratory, Texas A&M University, College Station, Texas (1986).
12. Salisbury, R. J., Stack, R., and Sassos, M. J., "Lubrication and Seal Oil Systems," *Proceedings of the Thirteenth Turbomachinery Symposium*, The Turbomachinery Laboratory, Texas A&M University, College Station, Texas (1984).
13. API Standard 617, "Centrifugal Compressors for General Refinery Service," Fifth Edition, (1988).
14. Atkins, K. E., Tison, J. D., and Wachel, J. C., "Critical Speed Analysis of an Eight-Stage Centrifugal Pump," *Proceedings of the Second International Pump Symposium*, The Turbomachinery Laboratory, Texas A&M University, College Station, Texas (1985).
15. Massey, I. C., "Subsynchronous Vibration Problems In High-Speed Multistage Centrifugal Pumps," *Proceedings of the Fourteenth Turbomachinery Symposium*, The Turbomachinery Laboratory, Texas A&M University, College Station, Texas (1985).
16. Black, H. F. and Jenssen, D. N., "Dynamic Hybrid Properties of Annular Pressure Seals," ASME Paper 71-WA/FF-38 (1971).
17. Allaire, P. E., Stroh, C. G, Flack, R. D., Kocur Jr., J. A., and Barrett, L. E., "Subsynchronous Vibration Problem and Solution," *Proceedings of the Sixteenth Turbomachinery Symposium*, The Turbomachinery Laboratory, Texas A&M University, College Station, Texas (1987).
18. Wachel, J. C., "Rotordynamic Instability Field Problems," Second Workshop on Rotordynamic Instability of High Performance Turbomachinery, NASA Publication 2250, Texas A&M University (1982).
19. Kirk, R. G. and Donald, G. H., "Design Criteria for Improved Stability of Centrifugal Compressors" Rotor Dynamic Instability, ASME Publication AMD-*55* (1983).
20. Kirk, R. G., Nicholas, J. C., Donald, G. H., and Murphy, R. C., "Analysis and Identification of Subsynchronous Vibration for a High Pressure Parallel Flow Centrifugal Compressor," ASME Journal of Mechanical Design, Paper No. 81-DET-57 (1981).
21. Wachel, J. C. and Smith, D. R., "Experiences with Nonsynchronous Forced Vibrations in Centrifugal Compressors," Rotordynamics Instability Problems in High-Performance Turbomachinery, NASA Publication 2338, pp. 37-44 (1984).
22. Fulton, J. W., "Subsynchronous Vibration of Multistage Centrifugal Compressors Forced by Rotating Stall," The Fourth Workshop on Rotordynamic Instability Problems in High-Performance Turbomachinery, Texas A&M University, College Station, Texas (1986).
23. Stroh, C. G., "Rotordynamic Stability—Simplified Approach," *Proceedings of the Fourteenth Turbomachinery Symposium*, The Turbomachinery Laboratory, Texas A&M University, College Station, Texas (1985).
24. Atkins, K. E. and Perez, R. X., "Assessing Rotor Stability Using Practical Test Procedures," *Proceedings of the Twenty-First Turbomachinery Symposium*, Turbomachinery Laboratory, Texas A&M University, College Station, Texas (1992).
25. Zeidan, F. Y., Perez, R. X., and Stephenson, E. M., "The Use of Honeycomb Seals in Stabilizing Two Centrifugal Compressors," *Proceedings of the Twenty-Second Turbomachinery Symposium*, Turbomachinery Laboratory, Texas A&M University, College Station, Texas (1993).
26. Sorokes, J. M., Kuzdzal, M. J., Sandberg, M. R., and Colby, G. M., "Recent Experiences in Full Load Full Pressure Shop Testing of a High Pressure Gas Injection Centrifugal Compressor," *Proceedings of the Twenty-Third Turbomachinery Symposium*, Turbomachinery Laboratory, Texas A&M University, College Station, Texas (1994).
27. Wachel, J. C., and Szenasi, F. R., "Analysis of Torsional Vibrations in Rotating Machinery" *Proceedings of the Twenty-Second Turbomachinery Symposium*, The Turbomachinery Laboratory, Texas A&M University, College Station, Texas (1993).
28. Tripp, H., Kim, D., and Moll, R. W., "A Comprehensive Cause Analysis of a Coupling Failure Induced By Torsional Oscillations in a Variable Speed Motor," *Proceedings of the Twenty Second Turbomachinery Symposium*, Turbomachinery Laboratory, Texas A&M University, College Station, Texas (1993).
29. Wachel, J. C. and Tison, J. D., "Vibrations in Reciprocating Machinery and Piping," *Proceedings of the Twenty-Third Turbomachinery Symposium*, The Turbomachinery Laboratory, Texas A&M University, College Station, Texas (1994).
30. VanLaningham, F. L. and Wood, D. E, "Fatigue Failures of Compressor Impellers and Resonance Excitation Testing," *Proceedings of the Eighth Turbomachinery Symposium*, The Turbomachinery Laboratory, Texas A&M University, College Station, Texas (1979).
31. Bultzo, C., "Analysis of Three Impeller Failures: Experimental Techniques Used to Establish Causes" *Proceedings of the Fourth Turbomachinery Symposium*, The Turbomachinery Laboratory, Texas A&M University, College Station, Texas (1975).
32. Sohre, J. S., "Steam Turbine Blade Failure, Causes and Corrections," *Proceedings of the Fourth Turbomachinery Symposium*, The Turbomachinery Laboratory, Texas A&M University, College Station, Texas (1975).